

PROCEEDINGS OF SPIE

SPIDigitalLibrary.org/conference-proceedings-of-spie

Planar optics enables chromatic aberration correction in immersive near-eye displays

Zhan, Tao, Zou, Junyu, Xiong, Jianghao, Chen, Hao, Liu, Sheng, et al.

Tao Zhan, Junyu Zou, Jianghao Xiong, Hao Chen, Sheng Liu, Yajie Dong, Shin-Tson Wu, "Planar optics enables chromatic aberration correction in immersive near-eye displays," Proc. SPIE 11310, Optical Architectures for Displays and Sensing in Augmented, Virtual, and Mixed Reality (AR, VR, MR), 1131003 (19 February 2020); doi: 10.1117/12.2542365

SPIE.

Event: SPIE AR VR MR, 2020, San Francisco, California, United States

Planar optics enables chromatic aberration correction in immersive near-eye displays

Tao Zhan^{*a}, Junyu Zou^a, Jianghao Xiong^a, Hao Chen^{ab}, Sheng Liu^c, Yajie Dong^{abd}, Shin-Tson Wu^a
^aCREOL, The College of Optics and Photonics, University of Central Florida, Orlando, FL 32816, USA; ^bNanoScience Technology Center, University of Central Florida, Orlando, FL 32826, USA; ^cGoerTek Electronics, Santa Clara, CA 95054, USA; ^dDepartment of Materials Science & Engineering, University of Central Florida, Orlando, FL 32816, USA;

ABSTRACT

We demonstrate an optical chromatic aberration correction method for virtual reality (VR) displays using cost-efficient flat optics. The fabricated ultra-broadband liquid crystal thin-film polymer lens is based on the Pancharatnam-Berry phase and manifests over 97% first-order diffraction efficiency over the display spectrum. By cascading the fabricated polymer lens with the conventional Fresnel VR lens, the lateral color breakup in the near-eye display system can be reduced by more than 10 times. Both optical designs and experimental results are presented and discussed.

Keywords: Planar optics, chromatic aberration, Pancharatnam-Berry phase, VR Optics, liquid crystal, metalens

1. INTRODUCTION

Recent developments in virtual reality technology, facilitated by high-pixel-density displays and robust mobile processors, have offered the unprecedented capability to immerse the viewer in a virtual world. VR has already proven its ability to transform how individuals and businesses interact with each other and their ecosystems. Despite how widely VR has been used for gaming, this technology is expanding to a plethora of applications, including but not limited to education, retail, and healthcare.

Although more than 10 million VR devices have been shipped since 2016, the imaging quality of current VR products is still not ideal when compared with that of the real world. Since compact and light-weight are always desired for head-mounted displays, currently only one singlet lens is employed in most of the commercial VR devices, making it quite stimulating to keep a decent imaging performance within the whole field of view (FOV), which is typically $>100^\circ$ for an immersive impression [1]. As a consequence, the color breakup, particularly at the edges of objects, can be observed due to chromatic aberrations (CAs) at the margins of the displayed image. Even though the significance of this effect is dependent on the image content and users' gaze point, it is still desirable to provide chromatic aberration corrections (CACs) for better user experience.

Digital CAC is commonly employed in existing VR devices. With extra graphics computation, the perceived CA can be substantially reduced by means of image pre-processing [2], where the digital image warping is applied to each color channel independently with distinctive coefficients determined by the viewing optics. With the correct subpixel digital corrections, the virtually separated RGB subpixels can be re-combined again. However, from the system perspective, the digital CAC still has several issues and may compromise the display performance:

1. Sub-channel aberrations. There is a range of wavelengths within each color channel, and each portion of it suffers from different lateral color shifts. Therefore, the digital CAC designed for the three RGB peak wavelengths cannot correct the CA in each color channel. This incapability would also degrade the accuracy of the color displayed.
2. Interpupillary distance (IPD) variation. Since the digital CAC is usually set for a fixed point in the eyebox, this method cannot offer the ideal correction for users with different IPDs.
3. Image rendering. Digital CAC would exaggerate the pressure for image rendering, which is already quite challenging for high-resolution and high-quality graphics in VR. To share the heavy burden on the graphic processing unit (GPU), a new display processing unit (DPU) has been developed to supporting digital CAC in VR [3].
4. Processing time. High framerate is usually required in VR devices for a small latency. The digital correction would occupy extra processing time in each frame, which can be even longer with a higher display resolution.

Therefore, the software-based digital pre-distortion is not an ideal solution to CA in VR displays at present. In this work, we demonstrate a hardware-based CAC approach using novel flat optics, a Pancharatnam-Berry phase lens (PBL) made of liquid crystal (LC) polymer that shows negative chromatic dispersion. After the hybridization of a plastic Fresnel lens and a PBL, the CA can be evidently reduced, as illustrated in Fig. 1. Firstly, the system configuration is determined by the sequential raytracing simulation. Then, the desired broadband LC lens is fabricated, characterized and then assembled with a plastic Fresnel lens as the achromatic viewing optics in our VR prototype. Finally, the CAC performance of the proposed system is experimentally evaluated, and its potential application in folded VR optics is also discussed.

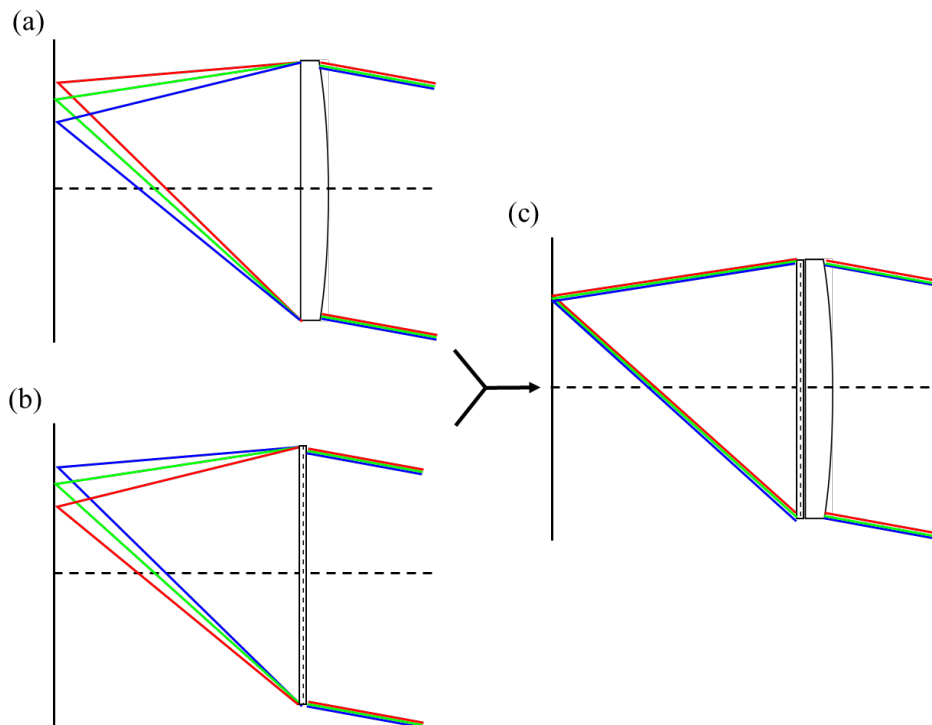


Figure 1. Illustration of transverse chromatic aberrations in a) a compact refractive Fresnel lens, b) a diffractive LC lens, and c) the proposed hybrid doublet exhibiting achromatic performance.

2. DESIGN

2.1 Liquid Crystal Flat Optics

The Pancharatnam-Berry phase optical elements (PBOEs) [4,5] proposed here can be understood as dielectric metasurfaces or patterned half-wave plates with in-plane spatial-rotating crystal axis, denoted as $\psi(x,y)$. With circularly polarized input, the corresponding Jones calculus can be established as [5]:

$$J_{out} = R(-\psi)W(\pi)R(\psi)J_{\pm} = -je^{\pm 2j\psi}J_{\mp}, \quad (1)$$

where

$$J_{\pm} = \frac{1}{\sqrt{2}} \begin{bmatrix} 1 \\ \pm j \end{bmatrix}, \quad (2)$$

$R(\Psi)$ is the rotation operation matrix, $W(\pi)$ is the phase retardation matrix representing the half-wave plate. J_{\pm} stands for the Jones vector of left- and right-handed circular polarized (LCP and RCP) light. It is shown that the half-wave plate results in not only a CP handedness conversion but also a $\pm 2\psi(x, y)$ phase delay. If the in-plane LC orientation rotates in a paraboloidal way, then a lensing wave-front can be structured to function as a PBL. Moreover, for a broadband application that can operate within the whole display spectrum, a tailored axial molecule orientation needs to be implemented, such a twist-homo-twist structure [6], as displayed in Fig. 2. In this three-layer design for broadband

performance, the first and third layer is made of LC polymer twisted with opposite directions by doping chiral dopants with opposite handedness, while the sandwiched second LC polymer layer is not twisted in the axial direction. This waveplate broadband operation principle was firstly proposed by Pancharatnam with cascaded discrete waveplates with premeditated orientation angles between their optical axis [7], then extended to waveplates with continuously rotating optical axis using twist nematic LC cells [8] and multilayer LC polymer films [9,10]. The proposed three-layer sandwich-like PBL should be able to cover the majority of the light spectrum of the LCD panel, which typically ranges from 430 nm to 680 nm. Additionally, from the material perspective, polymerizable LC material with minor or negative birefringence dispersion is ideal for a diminished variation of retardation over the display spectrum. However, these materials are relatively costly for applications in large-volume consumer gadgets at this stage. Thus, in this work, our PBL is fabricated using one of the most cost-efficient LC reactive mesogen material, RM257, although it has a relatively large birefringence dispersion that may hinder the broadband performance.

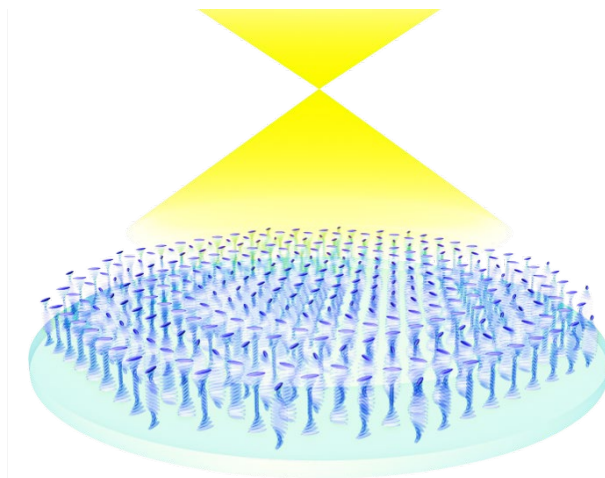


Figure 2. Schematic illustration of LC anisotropy axis orientation in the PBL with flat geometry and a twist-homo-twist structure for broadband operation.

2.2 Optical layout

The system structure of the proposed VR viewing optics is illustrated in Fig. 3(a). Compared to conventional VR optics, our design only added three thin films, including a quarter-wave plate, a PBL, and a circular polarizer, attaching negligible weight and volume to the existing system. The flat optical parts are positioned upon the Fresnel surface of the plastic lens for convenient alignment. Also, the PBL is positioned between the display and Fresnel lens, where the angle of incidence is smaller than after the Fresnel lens, leading to a higher diffraction efficiency at the PBL surface.

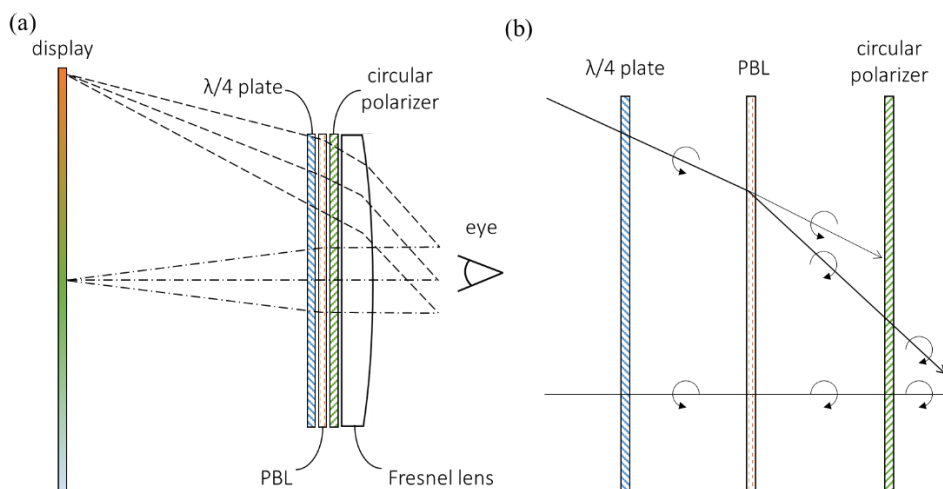


Figure 3. Illustration of (a) optical layout and (b) polarization state changes in the proposed VR viewing optics.

Figure 3(b) illustrates how the polarization state of display light varies through flat optical parts. The light emitting from the display panel is firstly converted from linear to circular polarization by a broadband quarter-wave plate. After passing through the PBL, the polarization handedness of the first-order diffracted light would be switched, as shown in Eq. (1), while that of the zero-order leakage remains unaffected. To block the stray light from the PBL's zero-order leakage, especially from oblique incidence, a broadband circular polarizer is inserted between the PBL and Fresnel lens. In this manner, only the desired light rays from first-order diffraction can go through the circular polarizer and enter the viewer's eye. If the light rays emitting from the display panel is unpolarized, such as those from micro-LED panels, then a polarization converter or a polarizer should be attached upon the panel to keep the polarization state of output light linear. There is no denying that this may cut half of the light efficiency, but in general, high brightness is not a necessity in VR displays.

2.3 Ray-tracing design

The phase profile or focal length of the PBL demands a tailored design for an optimized system imaging performance with the Fresnel lens. Generally, for achieving an optical CAC similar to the design of an achromatic double [11], the following restriction should be satisfied:

$$\frac{K_{Fresnel}}{V_{Fresnel}} + \frac{K_{PBL}}{V_{PBL}} = 0 \quad (3)$$

where K and V are the optical power and Abbe number of the Fresnel lens and corresponding PBL. As a type of diffractive lens, the Abbe number of PBL is unique since it is equal to -3.45, no matter what kind of LC reactive mesogen material it is made of. The Fresnel lens is made of polymethyl methacrylate (PMMA), whose Abbe number is around 58. Thus, the optical power of PBL should be ~16 times smaller than that of the Fresnel lens. In the next step, sequential ray-tracing simulation and optimization are applied using commercial software, OpticStudio™. The PBL is modeled as a holographic diffractive optical element with 100% first-order diffraction efficiency. Stray light caused by the leakage from the PBL diffraction is not included in this assessment.

Figure 4 provides a comparison of the polychromatic root-mean-square (RMS) spot radius of the Fresnel lens and proposed hybrid optics. In VR systems using the Fresnel singlet, three color channels are noticeably separated when the field is larger than 30°. Given the simulated results, the proposed hybrid lens can enhance the image sharpness by ~2.5 times, making the image much clearer from 0° to 50° field. In the meantime, at the 0° field, adding a PBL could make the RMS spot smaller than the according Airy disk, which is 5.6 microns in radius, rendering the system diffraction-limited on-axis. To quantitatively assess the CAC potential of PBL, lateral color shift is also estimated for the viewing optics with and without PBL compensation, as presented in Fig. 5. As expected, the PBL has the potential to diminish the lateral color shift of the Fresnel singlet by over 10 times within a 100° FOV.

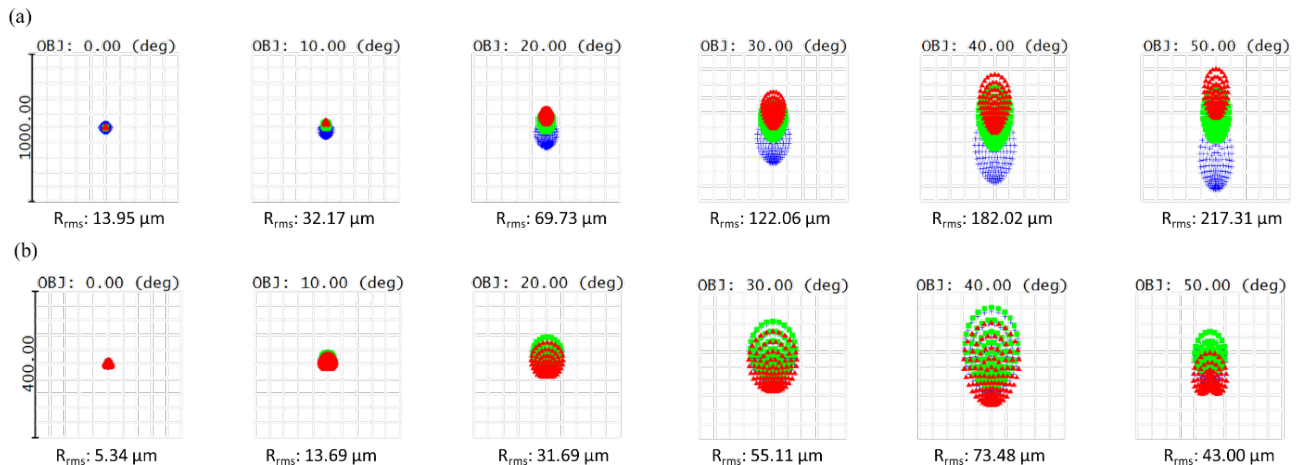


Figure 4. Standard spot diagram with RMS spot radius for (a) Fresnel singlet and (b) proposed hybrid optics. Color by wavelength, Red: 610nm, Green: 540nm, Blue: 450nm.

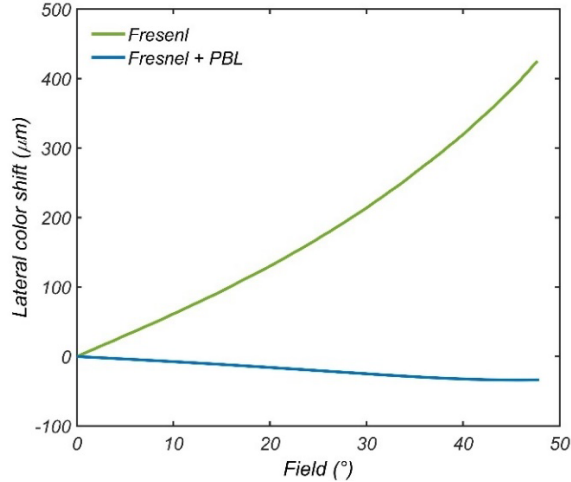


Figure 5. Standard spot diagram with RMS spot radius for (a) Fresnel singlet and (b) proposed hybrid optics. Color by wavelength, Red: 610nm, Green: 540nm, Blue: 450nm.

3. IMPLEMENTATION

The designed broadband PBL is fabricated based on the polarization holography photo-alignment method with multiple coating and curing processes [12]. Initially, a nanosized photo-alignment layer was created on a cleaned 2-inch-diameter glass substrate by spin-coating a 0.2 wt.% solution of Brilliant Yellow (BY) in dimethylformamide (DMF). The LC molecule orientation pattern for the designed lens profile was printed on the BY layer using polarization holography method. Then, four LC mesogen layers were spin-coated on the aligned surface one by one, while each coated layer was firstly polymerized by UV light centered at 365nm to form a solid surface and then provide alignment for the next layer. The fabricated PBL exhibits clear image quality and wide spectral bandwidth. The zero-order leakage is less than 3% over the display spectrum of the LCD panel, as plotted in Fig. 6.

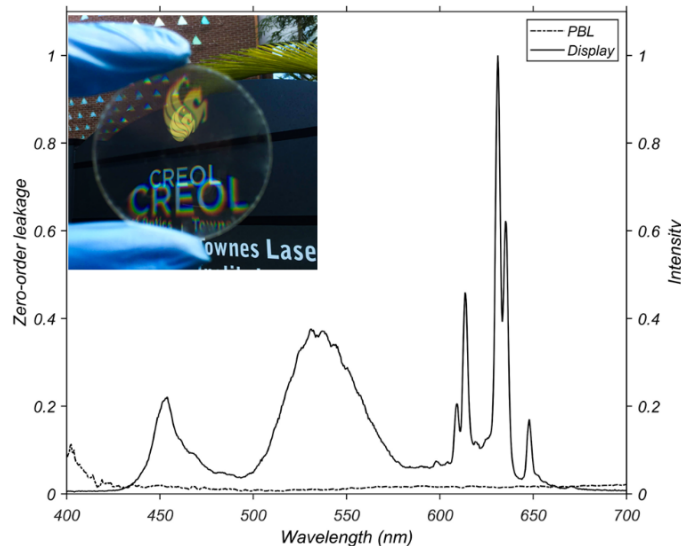


Figure 6. Measured zero-order leakage of the ultra-broadband PBL and the emission spectrum of the LCD displaying white light. Inside is a photo of the fabricated 2-inch PBL.

To demonstrate the CAC performance of the proposed hybrid lens, a colored image was displayed on the LCD screen without barrel distortion correction, which includes a set of evenly spaced bars with RGB segments, as plotted in Fig. 7. When viewing through the plastic Fresnel singlet, the test pattern bars are blurred, and the RGB colors are apparently displaced due to the transverse CA at peripheral FOV. When the proposed planar optics module, including a $\lambda/4$ plate, a

PBL and a circular polarizer, is attached to the Fresnel surface of the refractive lens, the color breakup at the periphery of FOV is significantly reduced. Fig. 8 shows another testing result with a black-and-white image. Utilizing the proposed optical architecture, the CA issue can be resolved at the expense of three planar optical elements without changing the compact form factor of the system.

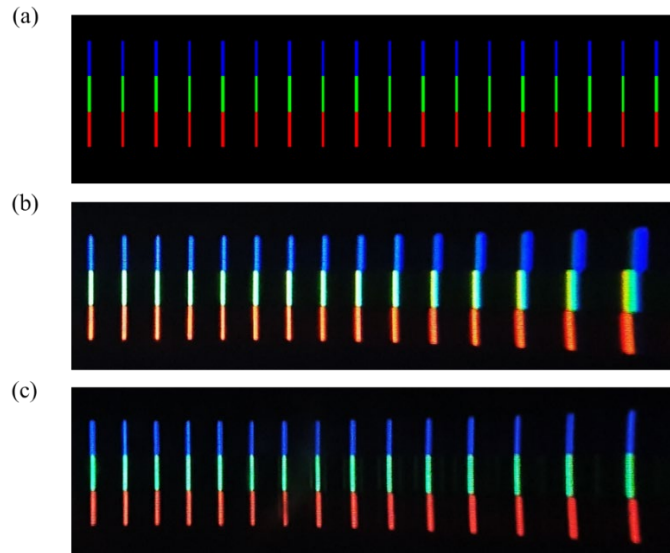


Figure 7. (a)Half-field CA testing pattern displayed on the LCD and the resulting images captured through the (b) conventional and (c) proposed viewing optics.

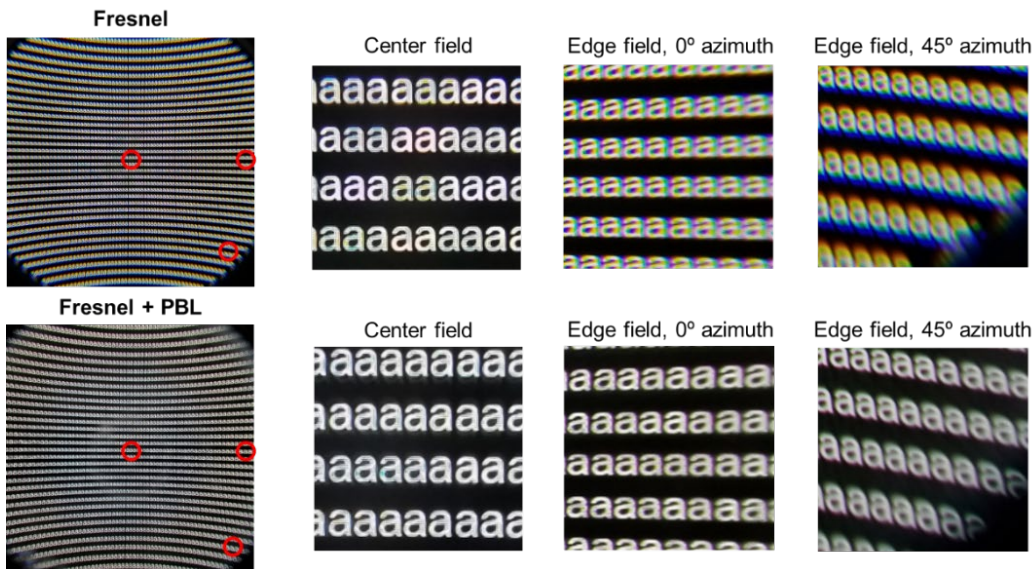


Figure 8. Full-field black-and-white image displayed on the LCD and the resulting images captured through the conventional and proposed hybrid viewing optics. The three enlarged parts are center field and edge fields at 0° and 45° azimuth from left to right.

4. PANCAKE LENS

The catadioptric pancake lens can provide decent image quality yet with a compact size for VR displays [13]. Figure 9(a) illustrate a simple example of this kinds of designs. The light rays emitting from the display panel pass through the first half-mirror and reflected by a reflective polarizer to the half-mirror. Then, the polarization state is switched when it is reflected by the first half mirror, such that it can pass through the reflective polarizer after traveling through the cavity

for three times. In these catadioptric systems, the on-axis reflector, which manifests no index difference for all wavelengths, could reduce not only the field curvature but also the CA. However, the CA still cannot be eliminated as long as there are functioning refractive optical parts.

The broadband PBLs fabricated in this work can offer optical CAC not only for Fresnel singlet, as discussed earlier, but also for the folded pancake VR lenses. Similarly, the CAC can be done simply by adding a custom PBL on the first surface of a pancake lens, as shown in Figure 9(b). According to the ray-tracing results plotted in Figure 10, the lateral color shift in the example pancake lens can be reduced by ~20 times with the help of a PBL.

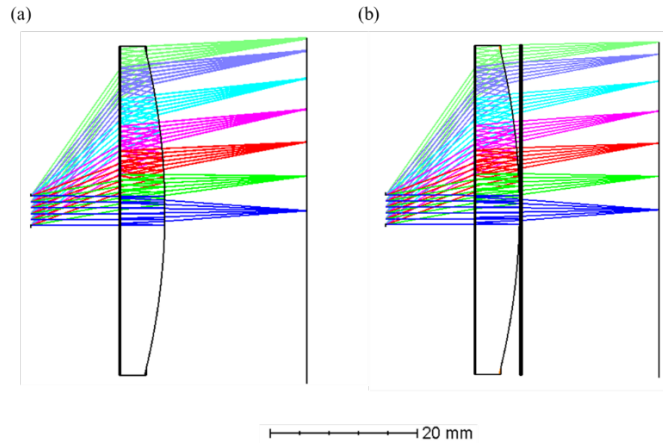


Figure 9. The optical layout of a pancake VR viewing optics (a) without and (b) with a PBL.

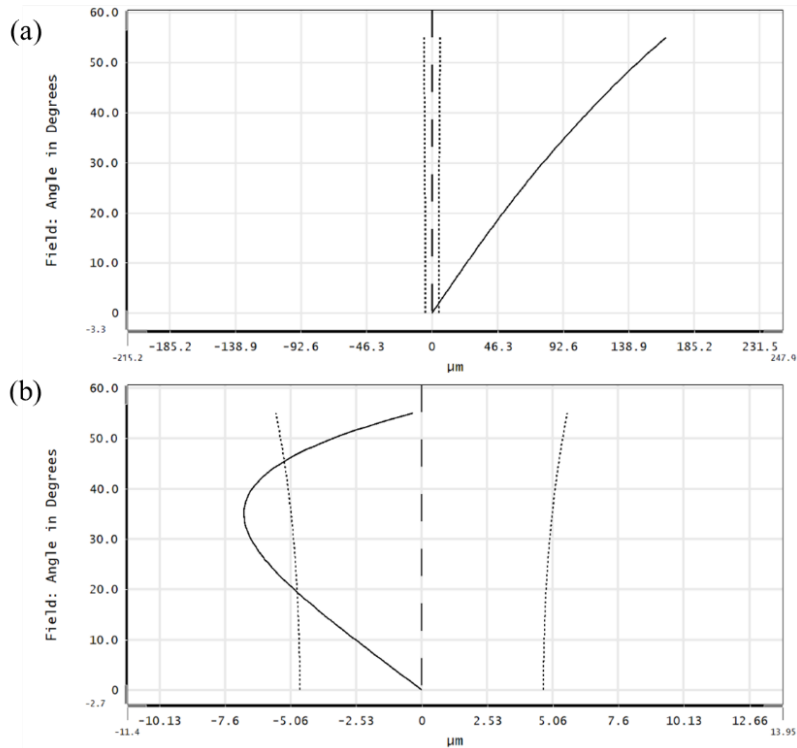


Figure 10. The lateral color shift of a pancake VR viewing optics (a) without and (b) with a PBL.

5. CONCLUSION

We have designed and demonstrated a prototype VR optical system with considerably reduced chromatic aberrations by utilizing planar optics based on the Pancharatnam-Berry phase. We fabricated the key optical element, an ultra-broadband planar polymer lens, manifesting high diffraction efficiency (>97%) over most of the visible spectrum. And due to the low-cost manufacturing of the planar polymer lenses and convenient additive adaptation from current VR devices, the proposed method and system has potential for widespread applications not only in the near-eye displays but also general imaging systems where chromatic aberration correction is desired.

REFERENCES

- [1] Wheelwright, B., Sulai, Y., Geng, Y., Luanava, S., Choi, S., Gao, W. and Gollier, J. "Field of view: not just a number," *Proc. SPIE* 10676, 1067604. (2018).
- [2] Brown, D. C., "Decentering distortion of lenses," *J. Photogramm. Eng. Remote Sens.* 32, 444-462 (1966).
- [3] Modrzyk, D., Martin, S., Crawford, A., Starkey, B., Vyas, K. and Unal, M., "Mira Display Processor for AR/VR Systems," *SID Int. Symp. Digest Tech. Papers* 50(1), 326-329 (2019).
- [4] Tabiryanyan, N., Roberts, D., Steeves, D. and Kimball, B., "New 4g optics technology extends limits to the extremes," *Photonics Spectra.* 51(3), 46-50 (2017).
- [5] Lee, Y. H., Tan, G., Zhan, T., Weng, Y., Liu, G., Gou, F., Peng, F., Tabiryanyan, N. V., Gauza, S. and Wu, S. T., "Recent progress in Pancharatnam-Berry phase optical elements and the applications for virtual/augmented realities," *Opt. Data Process. Storage* 3(1), 79-88 (2017).
- [6] Zhan, T., Lee, Y. H., Tan, G., Xiong, J., Yin, K., Gou, F., Zou, J., Zhang, N., Zhao, D., Yang, J., Liu, S. and Wu, S. T., "Pancharatnam-Berry optical elements for head-up and near-eye displays," *J. Opt. Soc. Am. B* 36(5), D52-D65 (2019).
- [7] Pancharatnam, S., "Achromatic combinations of birefringent plates," *Proceedings of the Indian Academy of Sciences Sect. A* 41(4), 130-136 (1955).
- [8] Shen, S., She, J., and Tao, T., "Optimal design of achromatic true zero-order waveplates using twisted nematic liquid crystal," *J. Opt. Soc. Am. A* 22(5), 961-965 (2005).
- [9] Oh, C. and Escuti, M. J., "Achromatic diffraction from polarization gratings with high efficiency," *Opt. Lett.* 33(20), 2287-2289 (2008).
- [10] Komanduri, R. K., Lawler, K. F. and Escuti, M. J., "Multi-twist retarders: broadband retardation control using self-aligning reactive liquid crystal layers," *Opt. Express* 21(1), 404-420 (2013).
- [11] Smith, W. J., [Modern Lens Design], McGraw-Hill Publisher, New York (2005).
- [12] Zhan, T., Zou, J., Xiong, J., Liu, X., Chen, H., Yang, J., Liu, S., Dong, Y. and Wu, S.T., "Practical Chromatic Aberration Correction in Virtual Reality Displays Enabled by Cost-Effective Ultra-Broadband Liquid Crystal Polymer Lenses," *Adv. Opt. Mat.* 1901360 (2019). DOI: 10.1002/adom.201901360.
- [13] Geng, Y., Gollier, J., Wheelwright, B., Peng, F., Sulai, Y., Lewis, B., Chan, N., Lam, W.S.T., Fix, A., Lanman, D. and Fu, Y., "Viewing optics for immersive near-eye displays: pupil swim/size and weight/stray light," *Proc. SPIE* 10676, 1067606 (2019)